

A Comparison of Laser Shearography and C-Scan for Assessing a Glass/Epoxy Laminate Impact Damage

Martin Kadlec · Roman Růžek

Received: 12 January 2011 / Accepted: 16 June 2011 / Published online: 16 July 2011
© Springer Science+Business Media B.V. 2011

Abstract Impact damage is a serious damage mechanism in composite materials, which limits their performance and reliability. Impact damage can occur during in-service applications or as a result of handling during manufacturing. Methods used currently for damage detection are based on different principles, and for that reason, they give a range of results no matter what the real damage is. Therefore, a comparison of the internal real damage with the flaw indications of a glass fibre-reinforced polymer (GFRP) laminate made with two non-destructive technique (NDT) methods has been investigated. Laser shearography measurements and C-scan ultrasonic detection were compared. Metallographic examination and surface indentation measurements provided information about the character of the real damage. Such a comparison has not yet been published because laser shearography is considered a qualitative technique. Each NDT method was able to visualise a different type of damage. The knowledge of the applicability of these methods is the key to taking advantage of both methods by combining their respective strengths. In terms of the reliability, simplicity and rapidity of all of the mentioned techniques, laser shearography turned out to be the most suitable method for the detection of barely visible flaws. The C-scan was more appropriate for precisely defining the inner damage. The tested material was a laminate typically used for ultralight aircraft. Information about the extent of damage is very important for airplane certification and maintenance.

Keywords Polymer matrix composite · Impact damage · Laser shearography · C-scan · Aerospace vehicles

1 Introduction

The expanding market of fibre-reinforced polymer composites for aerospace applications increases the need to identify damage that can radically decrease a material's performance.

M. Kadlec (✉) · R. Růžek
The Aeronautical Research and Test Institute (VZLÚ), Beranových 130, 199 05 Prague, Czech Republic
e-mail: kadlec@vzlu.cz
URL: www.vzlu.cz/en/

The variety of damage types is dominated by delamination. However, other types of heterogeneities caused at the manufacturing level or during in-service applications can also reduce the greatly exploited specific mechanical properties of composites [1, 2]. The different types of impact damage that occur can be divided into two basic categories—VID (visible impact damage) and BVID (barely visible impact damage). VID flaws can be detected by a general inspection and often without any special devices. Meanwhile, BVID flaws are very rarely detectable without using special equipment. These BVID flaws are often defined as millimetre deep dents. Some laboratories and manufacturers use slightly different values. For example, Boeing Design Criteria for Damage-Tolerant Carbon Fibre–Reinforced Polymer (CFRP) [3] defines BVID as small damage that may not be found during heavy maintenance general visual inspections using typical lighting conditions from a distance of 1.5 m. Typical dent depths fall in the range of 0.25 to 0.5 mm.

Impact induces delaminations at various interfaces distributed throughout the thickness. Most delamination defects are distributed in deep locations, especially at $h/3$ and $h/2$ [4] for a laminate thickness h , where $h=0$ for the impacted surface. The distribution through the depth can be compared to the frustum of a cone [5]. After the maximum delamination, the delamination defect size again decreases with depth. The total distribution of the damage as a function of depth can be modelled as two frusta of a cone with the maximum delamination as the common base. The extent of the damage is affected by a large number of parameters, such as nose shape and mass of impactor, impact velocity, types of fibre and matrix, interfacial treatment, fibre volume fraction, layup, laminate geometry, boundary condition and even pre-stress [6]. It is very difficult to determine the correlation between impact energy and delamination damage when the effect of each of these parameters is considered.

The energy-based approach is more suitable to determine the extent of damage than a force-based approach [7]. However, the use of kinetic energy as the impact parameter has disadvantages for large-mass (low-velocity) impacts because delamination damage varies with transverse plate stiffness, which is a function of plate size and the boundary conditions [8]. A complete energy balance for the impact of FRP laminates includes three major energy terms: the energy stored elastically, the energy absorbed in the creation of matrix damage and the energy absorbed in the creation of fibre damage. There are also two smaller terms: the energy of permanent indentation and a system loss term.

All non-destructive techniques (NDT) are limited by time and costs. Inspection techniques must be rapid and reliable. This paper deals with one of the most widespread techniques, the ultrasonic method, and with another method that is quickly being adopted, laser shearography. The aim of the paper is to evaluate different aspects of these methods from the point of view of real defect detection, BVID detection and inspection time. The presented NDT for planar inspection use different techniques, and they are therefore able to evaluate the state of a material in different ways. To ensure the safety of the structures, it is necessary to be able to evaluate the real damage.

The ultrasonic method is the classic and most widespread method used for delamination detection in a Carbon Fibre–Reinforced Polymer (GFRP) laminate [9]. Conventional ultrasonic investigation used for NDT is based on observations of the amplitude and the time variations of the mono-frequency input [10]. Another approach to NDT is based on an analysis of the non-linear response induced by flaws when using spectral data to detect and localise damage [11]. An alternative technique called Thermosonics (or Sonic IR) [12] is also used to identify and locate impact damage. In contrast to pulse thermography, this method is based on the observation of damage while the material is heating up. This is accomplished by exciting the sample with a short pulse of high-energy ultrasound radiation while an IR camera monitors the sample.

Laser shearography is still not a widely used NDT, but it provides many advantages in terms of very fast and full-field detection. A detailed description of the shearography principle and its interpretation can be found in references [13] and [14]. The stressing techniques needed for interferometric measurements of the loaded state are still being developed. A classic method uses thermal heating. One of the most recently researched techniques is impulsive thermal stressing by Xenon flash lamps [15]. Vibration excitation shearography has been studied as well [16].

Impact damage is a classic type of flaw that is detectable by shearography or other interferometric methods. The authors of reference [17] determined that the interferometric electronic speckle pattern (ESPI) method was able to identify the presence of impact damage, with the efficiency dependent on the through-thickness location of the delaminations produced by impact. The adoption of the ESPI technique, which is applicable to shearography, allowed significant reductions in inspection times, but quantitative estimates of the impact damage were drastically impaired by the high level of speckle noise typical of the technique.

Laser shearography is widely used for aerospace structures. Reference [18] describes one of the first industrial installations of laser shearography in Europe, a fully automatic inspection system for helicopter rotor blades. Entire rotor blades can be inspected within 10 minutes for delamination and debonding in the composite structure. Reference [19] described a few examples of applications in the aerospace industry that make use of NDT for composites, e.g., GLARE panels, honeycomb structures and glass (or carbon) fibre-reinforced plastics. The authors of reference [20] used laser shearography NDT to inspect wind turbine blades. The shearography technique was able to provide consistent documentation of the damage growth under fatigue loading of a honeycomb structure with a carbon/epoxy skin [21].

Several works compare various NDTs. Reference [22] compared shearography with C-Scan detection for carbon fibre-reinforced sandwich panels. The authors of reference [23] made an extensive comparison of shearography and active thermography. Another comparison of three different NDTs—electronic speckle pattern interferometry (ESPI), shearography and ultrasonic C-scan—for inspecting damaged laminate composites was made in reference [24]. Reference [25] compared ESPI and laser shearography and stated that both methods are able to detect the location of circular defects and to partially detect the severity of the defect. Reference [26] assessed laser shearography and the C-scan technique for the detection of high-velocity impact defects in advanced composites. Because of the low contrast of shearograms, no quantitative results were presented.

All of the mentioned papers deal with surface measurements. A comparison of detected signals and flaw sizes has not yet been conducted from the point of view of the real inner damage based on fractographic studies. Laser shearography is considered a qualitative technique. This paper investigates the possibility of conducting a quantitative evaluation of impact damage using laser shearography.

2 Experimental Procedures

2.1 Material and Impact Test Setup

A glass fibre-reinforced polymer laminate with an epoxy matrix that was 3.5 mm in thickness was used. The laminate had the following orientation of the 8H satin weave fabric: [0/45/90/0/45/0/90/45/0]. There was one more plain weave 0° layer on each surface.

This 11-ply laminate was cut into 9 rectangular specimens. The specimens were impacted by a 16 mm diameter, 5440 g mass impactor with energies from 5 to 40 J, which correspond to impact speeds of 1.36 to 3.83 m.s⁻¹, respectively. The energy values of impact were chosen based on the impact threats for aircraft structures that can arise from different causes, such as falling tools (4 J), runway debris (12–22 J) or hail impact (30–35 J) [27].

This configuration is considered a large-mass dynamic impact loading. The velocity detector was adjusted to measure the velocity just before the nose struck the specimen. Multiple impacts were prevented. The laminates were clamped vertically by a plate with a hole. Figure 1 shows the experimental setup for the impact test.

2.2 Residual Impression Measurement

Residual impressions can barely be detected in practice by a classic visual inspection, especially when the damage can be classified as BVID. It is generally assumed that indentations with depths less than 1 mm belong to this group. The surfaces of the indentations were scanned with an indicator gauge with a resolution of 0.01 mm. These contact measurements of the *z* axis (depth) were recorded over the line going through the middle of the dents. In addition, some specimens were measured in more detail over the whole area around the dent with a grid size of approximately 1 mm. The dent profile size was evaluated by applying 5% gradient lines to the edges of the dent. An indentation diameter was determined from the distance of the two intersection points defined by the supporting lines and the dent profile (Fig. 2).

2.3 Laser Shearography Measurements

A damaged area inspection with the laser shearography is based on an optical measuring technique, which uses coherent light for an interferometric inspection of materials. A sample is illuminated by a laser and visualised on a CCD camera via a special optical shearing element. The shearing element makes a coherent superposition of two laterally displaced images of the surface. The displacement is called a shear. The superposition of the

Fig. 1 Impact machine set-up with a clamped specimen between 2 boards

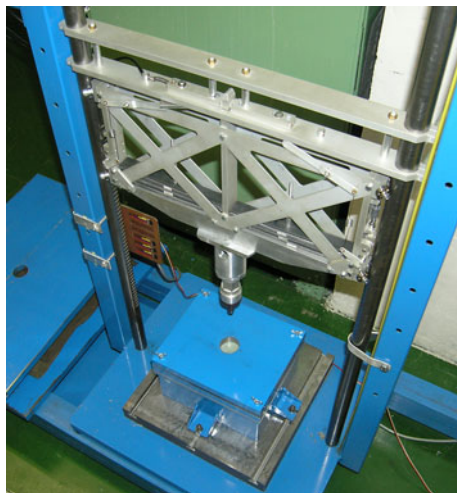
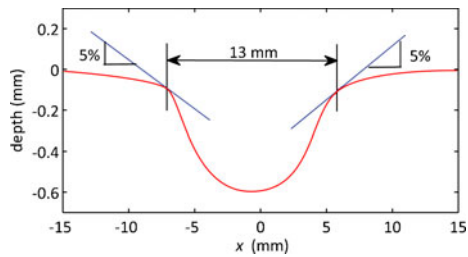


Fig. 2 Evaluation of an indentation diameter from a dent profile curve



two images is called a shearogram; it is an interferogram of an object wave with the sheared object wave as a reference wave. Figure 3 explains the measuring procedure.

A Q-800 Dantec Dynamics system with ISTR software was used for the data measurements and the evaluation. The apparatus was configured as follows: Two laser diodes (2×70 mV) with a wavelength of 653 nm were attached to the shearographic sensor, which had a resolution of 1392×1040 pixels (px). The camera had a Tokina 6–15 mm lens with an opened aperture of $f/1.4$. The shear angle and distance were adjusted to 0 degrees and 50 px.

The method has a maximum sensitivity as high as holography. The sensitivity is approximately proportional to the shear distance when the shear distance is relatively small [28]. The measuring sensitivity of the Q-800 is $0.03 \mu\text{m}/\text{shear distance}$, which can be calculated as $0.03/(50/1392)$ with the used shear base distance of 50 px. The theoretical sensitivity was $0.83 \mu\text{m}$. The filtering used significantly reduced the sensitivity, as will be explained further.

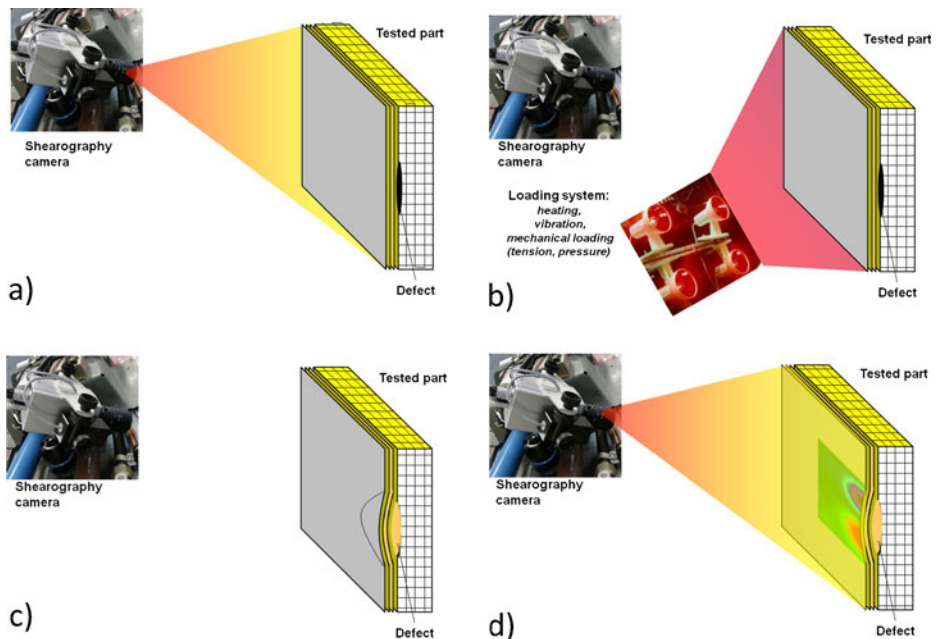


Fig. 3 Principle of shearography: **a** reference image is taken, **b** tested part is loaded, **c** unloading induces deformations and **d** images are superposed with the reference image

The specimen was loaded by heating with a 500 W lamp (OSRAM halogen lamp light bulb 500 W R7S 64706) from a distance of 30 mm for at least 20 s. The dents with depths below 0.1 mm had to be loaded by heating for 80 s, which will be described further at a later point in the text. The changing deformation state induced by thermal contraction in the gradually cooled specimen was measured several times over the course of a few minutes.

The recorded interferograms of any of the recorded states can be compared and doing so produces fringe patterns. It turned out to be essential for maintaining the low noise level to use the last interferogram from the measurement series as the reference image. The pattern can be recalculated into a deformation gradient. Around a thermally loaded flaw, this gradient is indicated by a typical “butterfly pattern”. The shear base distance should be subtracted from the indicated flaw size measured on the butterfly pattern (Fig. 4).

The image can be improved by filtering the low and/or high frequencies directly with the software. The low-pass filter determines the smallest details that are visible or how much the result is smoothed. For the experiment, 10 px width of the Gaussian filter was used, which corresponded to 1 mm. The high-pass filter removes information with low frequency or large fluctuations, such as a rigid body movement or bending. More information is removed for smaller parameter values. For this experiment, 200 px was used, which corresponded to 20 mm.

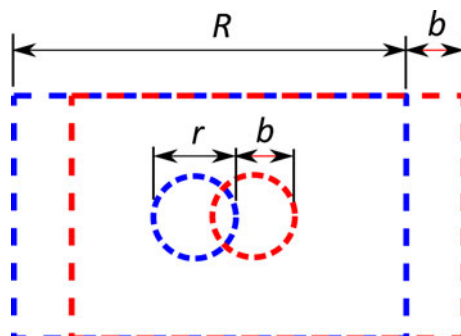
2.4 Ultrasonic C-Scan Measurements

An ultrasonic C-Scan method was used to obtain the damage distribution of the cumulative damage state. The method makes use of a manipulator with an ultrasonic probe in immersion liquid and scans a topologic surface of the sample. Omniscan MX OMNI-P-PA 16128 connected to a PC was utilised to evaluate the results. Phased array 3.5L64 NW1 3.5 MHz Probe was used. The gate position and the threshold level were set to 25 and 40% of the screen size, respectively. All the quoted C-scan images are shown in the amplitude visualisation. The measurements were performed in the Department of Composite Product Centre in Letov letecká výroba, s.r.o. in Prague.

2.5 Metallographic Examination

All of the specimens were cut by an IsoMet 4000 saw with an IsoCut CBN blade that was 0.63 mm in width. The blade velocity was 3450 rpm. A cut perpendicular to the surface was made in a small distance from the middle of the dent. The transparent epoxy metallographic mounting resin Ecoplast was used to mount the specimens. Automatic

Fig. 4 Recalculation of a flaw indication size ($r + b$) by subtracting shear b



grinding was performed with SiC P320 paper until reaching the marked line on the axis of the dent. The MetaDi suspension with 9-, 6- and 3-micron particles was used for automatic polishing. The Masterprep Polishing Suspension (0.05 μm) was used for the final stage of polishing. An ultrasonic cleaning was performed between the polishing steps. The metallographic microscope OLYMPUS GX 51 was utilised to evaluate the damage. Images were recorded with the ARTRAY Artcam 300MI camera. Observed cracks were marked on the recorded images, and then, the maximum horizontal distance between any of the cracks of a specimen was measured to obtain an inner damage range. It is necessary to state that the measured maximum crack extent depends on the cut location of a damaged sample. The centre lines of dents were carefully marked and the corresponding cut planes reached by polishing.

3 Results

The residual impressions after impact were measured. Figure 5 shows the typical surface shape of the 35 J dent, which was approximately 2 mm deep. The rest of the dents were measured in a line parallel to one of the specimen's edges. The dent profiles for different impact energies are demonstrated in Fig. 6. The diameter of the indentation area is determined on the basis of these profiles with the 5% gradient edge. The indentation depth was measured as the minimum value of a dent profile. Dent depths show a general rising trend with increasing of peak energy. The depth values vary from 3.4 mm for the 40 J dent to less than 0.1 mm for 5 J dents. The 35 and 40 J dents were substantially deeper than the rest of the dents formed with lower damage energies. This occurred because the laminate was 3.5 mm in thickness, and there was not enough supporting material for the damage to be absorbed. These values are summarised in the first part of Table 1. The deformation profiles also include the diameters of the indentation areas measured using the 5% gradient supporting lines. The maximum damage diameters vary from 6 to 19 mm as a function of the impact energy. These values are shown in the same table.

Laser shearographic measurements were performed for all of the dents. The standard loading involved a 20 s heating time. This approach provided indications of the dents

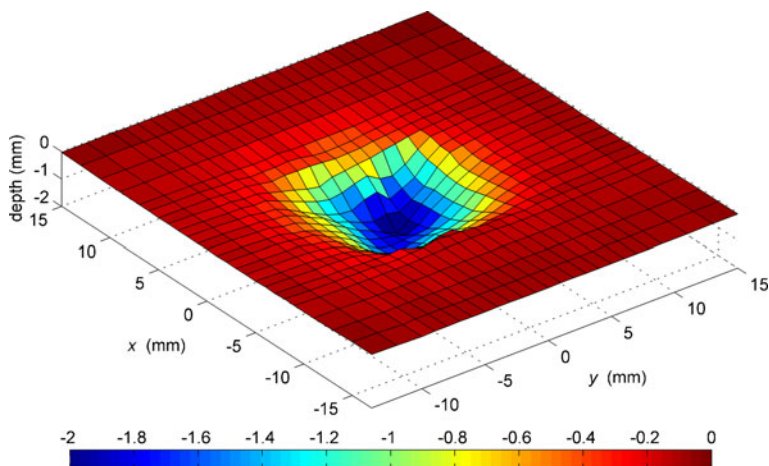
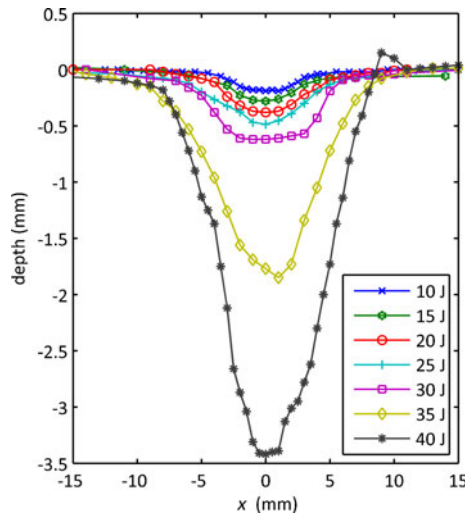


Fig. 5 Residual impression of a 35 J dent

Fig. 6 Dent profiles of laminates impacted by various energies. The laminate was 3.5 mm thick



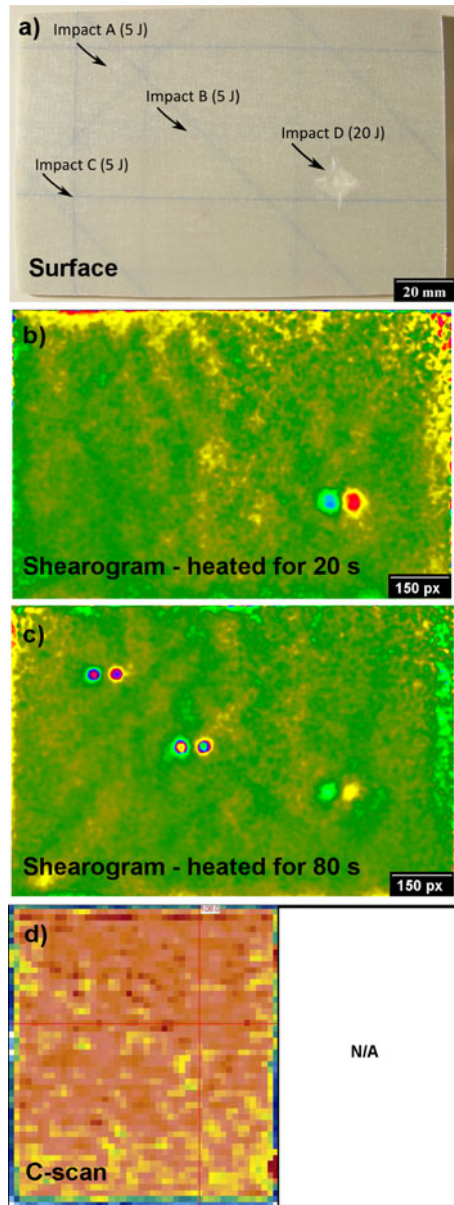
visualised by the typical butterfly pattern for all of the dents, except for one of the 5 J dents. The indicated sizes with the subtracted shear are presented in Table 1. The sizes vary between 5 and 20 mm and are comparable with the indentation areas, as will be further described later. A C-scan was performed on specimens impacted by 5, 15, 25 and 40 J energy. The values of the indicated sizes are shown in Table 1. On the one hand, the C-scan indications are significantly higher than shearography indications for the high-energy dents, mainly for VID flaws. On the other hand, low-energy damage was not indicated at all by the C-scan method for the used parameters. The results for two selected specimens are demonstrated in the following paragraphs.

The shearography evaluation of the indentations can be influenced by heating time, which causes different rates of deformation. Figure 7a presents a specimen damaged by three 5 J impacts and one 20 J impact. Additional interferograms under different loading

Table 1 The measurement results including indentation depth, maximum damage diameter and flaw indication sizes for laser shearography and C-scan detection

Impact Energy (J)	Indentation depth (mm)	Maximum damage diameter (mm)		Indicated size (mm)	
		Indentation area (5% grad. edge)	Inner damage	Shearography	C-scan
5 (A)	<0.1	N/A	N/A	5.2	0
5 (B)	<0.1	N/A	N/A	5.9	0
5 (C)	<0.1	N/A	2.4	0	0
10	0.21	6.5	12.7	8.6	N/A
15	0.28	7	19.2	12.1	17
20	0.38	9	20	12.8	N/A
25	0.49	11.5	23	13	22
30	0.61	13	27.5	15.8	N/A
35	2.03	17.5	28	20.1	N/A
40	3.37	19	30	19.9	32

Fig. 7 **a** Impacted specimen surface with 4 dents where 5 J damage is not visible, **b** phase image of this specimen heated for 20 s, **c** another phase image of this specimen heated for 80 s where even some 0.1 mm deep dents can be detected, **d** ultrasonic C-scan of the corresponding area in amplitude visualisation



conditions were obtained for this specimen. The first measurement was performed after 20 s of heating (Fig. 7b). In this case, only the 20 J impact was indicated. Then, 40 s of heating was performed with the same result. Finally, 80 s of heating was applied to increase the deformation gradient even more. This intensive loading indicated two of the three 5 J dents, which were less than 0.1 mm deep (Fig. 7c). This image was recorded several seconds after heating when the temperature decrease was sufficiently fast. However, the measurement of the intensive deformation gradient reduced the visibility of the 20 J damage pattern.

Some of the specimens were measured with an ultrasonic C-scan, which provides a topological image of the laminate. The discussed four-dent specimen was used. Because other kinds of specimen evaluations were also done, only the left part of the specimen with 5 J dents was measured (Fig. 7d). The C-scan did not detect any of these 5 J indentations for the used parameters.

The second examined specimen was damaged by a 15 J impact (Fig. 8a). The phase image of the shearogram indicated a dent with the typical pattern (Fig. 8b). An ultrasonic C-scan provided a topological image that revealed the delamination of the 15 J damage (Fig. 8c).

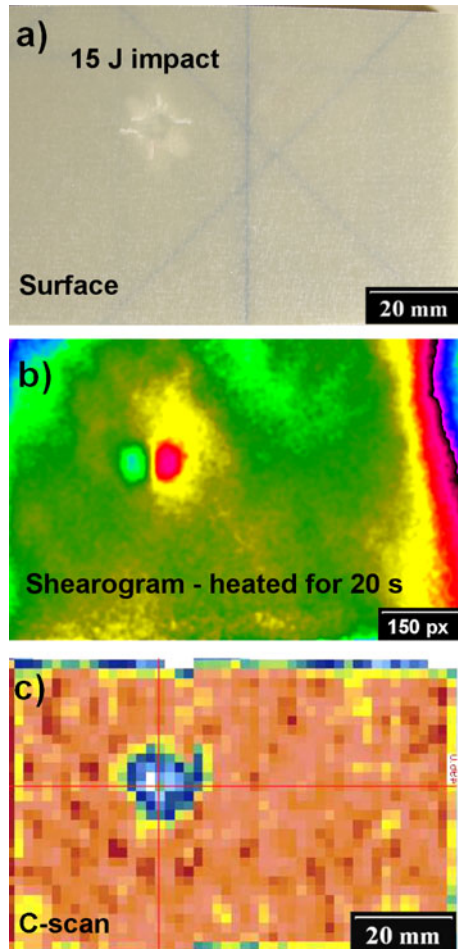
A metallographic examination in a bright field illumination was performed on cross-sections of the dents. The maximum range of the damaged area on the cuts was measured and is noted in Table 1 as the inner damage. Figure 9a shows the cross section of a 5 J impact location with minor ply cracks (matrix microcracking) in $\pm 45^\circ$ tows. A void due to entrapped air is shown in the inter-ply region. Both the specimen surfaces are coherent. Figure 9b shows the 10 J impact site with multiple ply cracks and delaminations on the non-impacted (back) side of the laminate. Most of the observed delaminations can be characterised as adhesive failure at the fibre (tow)-matrix interface. Fibre fracture is visible in some 0° plies. The impacted (front) side for up to 1/3 of the specimen depth is undamaged in the centre. Only delaminations along 0° tows are apparent further from the centre. Figure 9c presents the 15 J impact location. The damage character is similar to the 10 J impact, but the area has a higher extent of delaminations, and the undamaged area below the indentation is reduced. A void induced by impact damage is apparent. The back surface of the laminate is broken which is the case for all of the specimens impacted by energies greater than 15 J. Figure 9d shows the 20 J impact site. The damage consists of delaminations and microcracks along and within tows that spread through the whole thickness of the specimen. The cracks are connected to the extended formation. Fibre fracture along the vertical axis is apparent. The indented surface is still coherent. Figure 9e displays the 25 J impact location. Delaminations are widely opened and extend to larger distances from the indentation area. Fibre fracture occurs throughout the thickness. The front surface is not broken through. Figure 9f shows the 30 J impact in which both the front and back surfaces are breached. Transverse cracks in the resin-rich areas connect horizontal cracks along adjacent plies.

Figure 10 summarises the results of the damage indications compared with the real damage state and the indentation area diameter. Circular points correspond to the inner metallographic results, dagger-shaped points correspond to the indentation area diameter and the remaining points represent the C-Scan and shearography results. The inner damage diameter plotted against impact energy can be fit by a logarithmic curve. The same can be done for the C-Scan values. The curves have very similar parameters. It can be stated that the ultrasonic C-Scan method evaluated the real damage effectively. The shearography indications and the diameter of the indented surface can be fit by a linear relation. It can be concluded that shearography is the most suitable method to detect surface residual indentations. Moreover, the measurements are very rapid, and the technique is capable of detecting even the smallest damage from a 5 J impact.

4 Discussion

A plot of projected delamination damage and impact energy for a thickness of 3.6 mm for quasi-isotropic CFRP T300/914 laminate was published in reference [5]. One range represented the energy up to 6 J in which there was no damage. All of the energy was

Fig. 8 **a** Impacted specimen surface with a 15 J dent, **b** phase image of this specimen heated for 20 s, **c** ultrasonic C-scan of the corresponding area in amplitude visualisation



absorbed through elastic deformation. This fact corresponds with the submitted results in which negligible inner damage was found for the impact energy of 5 J. Nevertheless, laser shearography was capable of detecting this damage as a surface impression. Additional significant evidence for the existence of a delamination threshold load for low-velocity impact loading on composite laminates has been presented [29]. In general, the tougher the matrix and the stronger the interface, the less damage is expected. At elevated temperatures, however, the matrix resin becomes so soft and compliant that it cannot withstand an impact event that would not normally cause damage at room temperature [30, 31].

According to reference [5], the range of energies from 6 J onward was absorbed during the creation and propagation of damage, in addition to the elastic deformation. In this phase, the delamination damage increased very rapidly with the increase in impact energy. The damage distribution moved its maximum towards the opposite side of the laminate. Our metallographic results confirm this fact. This effect makes it clear that the shearography technique underestimates the size of the inner damage as a function of the impact energy, which moves the peak of damage further from the surface.

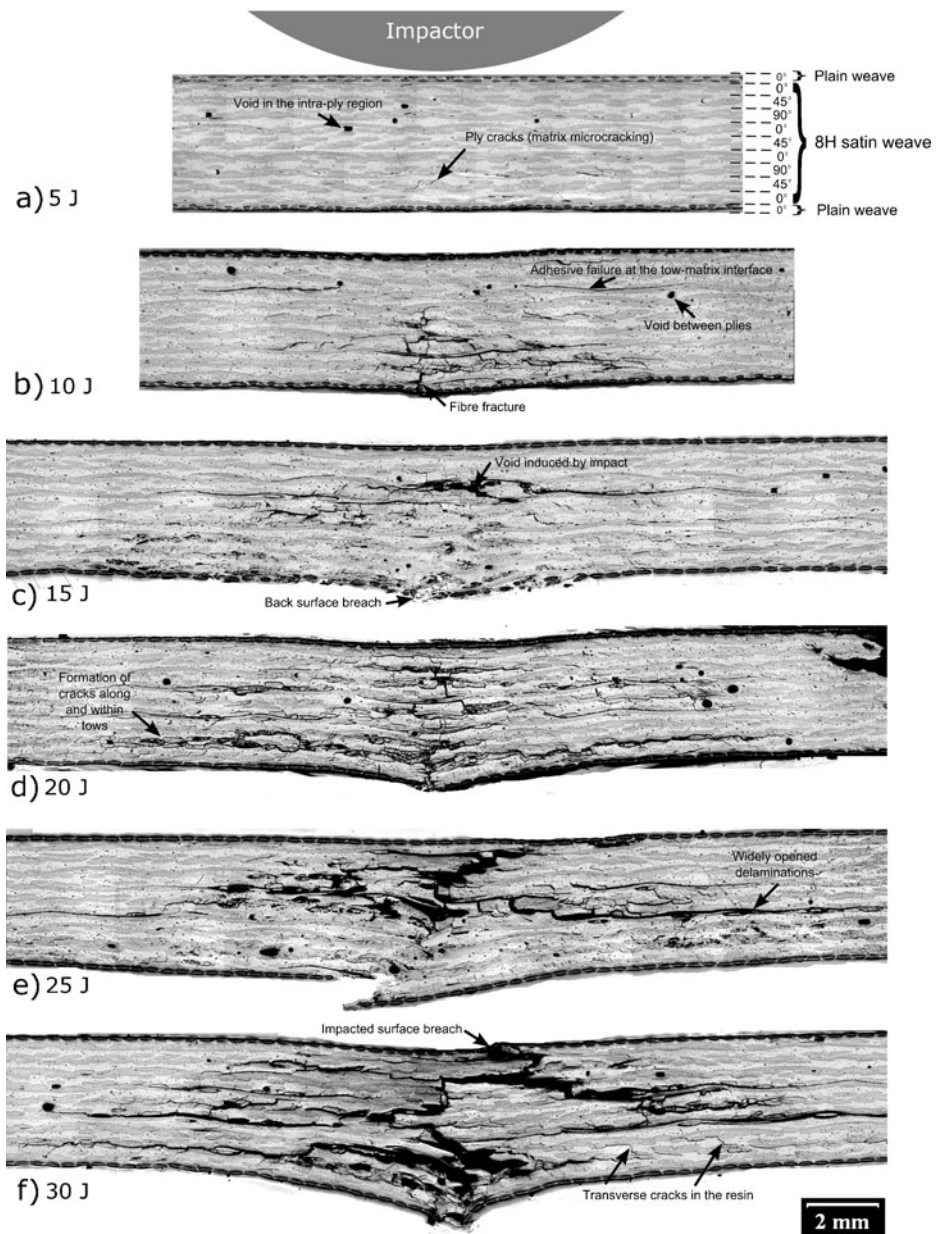
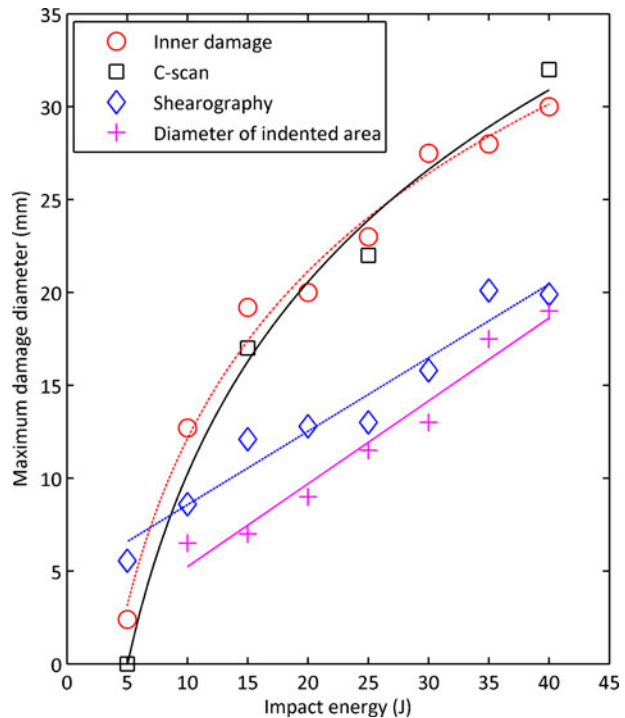


Fig. 9 Cross-sectional photographs of the woven glass fabric laminate in a bright field illumination. Observed damage for various impact energies is described

The C-scan technique detects inner damage effectively. However, it is not able to detect small damage from 5 J impacts for the given material configuration. The ultrasound techniques detect discontinuities within a part or structure by means of a reflection. If none of the contacts between plies have failed and only surface deformation is present, this technique is unable to detect this small flaw. The metallography confirmed that this 5 J

Fig. 10 Comparison of the maximum diameter of the inner damage, the indented surface area and the detected flaw indications with two NDT techniques—the ultrasonic C-scan and laser shearography



damage causes only negligible inner damage, so it was not indicated in the ultrasound. This is the reason why C-Scan cannot detect small BVID flaws. The C-scan method can be also very time consuming since a 2-D robotic carriage system is required for scanning [32].

5 Conclusion

Two different NDTs have been compared to evaluate their ability to detect real inner impact damage in glass fibre–reinforced laminates. A metallographic evaluation was performed to determine the real state of the material. Moreover, the residual impression after impact was measured.

To conclude, laser shearography detects the surface residual indentation and reacts to surrounding damage. Even small damage from a 5 J impact that causes 0.1 mm deep dents with negligible delamination can be detected by laser shearography. This surface deformation can lead to a decrease in the toughness of construction, which may result in a reduced bearing capacity. In contrast, the VID results are undersized, and the sensitivity decreases with the flaw depth. The minimum detectable size of delamination could not be stated because the surface indentation rapidly develops the indication pattern, which overlaps the indication of any small inner damage.

Laser shearography is a rapid method for the detection of any surface damage that can then be analysed with other NDT techniques to obtain the real inner state of the material. It is important to consider that, in this paper, the defined relationship between BVID, VID, and impact energy is limited to the boundary conditions used during the damage realisation, and the relationships can be different. All of the other statements are generally valid for GFRP.

Acknowledgments The authors would like to thank the Department of Composite Product Centre in Letov letecká výroba, s.r.o. in Prague for the C-Scan measurements. Financial support of grant MSM 0001066903 from the Czech Ministry of Education, Youth and Sport is also gratefully acknowledged.

References

1. Pitarresia, G., Founda, M.S., Patterson, E.A.: An investigation of the influence of macroscopic heterogeneity on the thermoelastic response of fibre reinforced plastics. *Compos Sci Technol* **65**, 269–280 (2005)
2. Thouless, M.D., Jensen, H.M., Liniger, E.G.: Delamination from Edge Flaws. *Proc R Soc London A* **447**, 271–279 (1994)
3. Fawcett, A.J., Oakes, G.D.: Boeing composite airframe damage tolerance and service experience. DA ETSI Aeronáuticos, Spain. [http://www.dmpa.upm.es/UserFilesQM/File/2009/Composite Damage Tolerance Maintenance Boeing.pdf](http://www.dmpa.upm.es/UserFilesQM/File/2009/Composite%20Damage%20Tolerance%20Maintenance%20Boeing.pdf) (2006) Accessed 22 June 2010
4. Fu, H., Zhang Y.: On the distribution of delamination in composite structures and compressive strength prediction for laminates with embedded delaminations. *Appl Compos Mater*. doi: 10.1007/s10443-010-9154-y
5. Hosur, M.V., Murthy, C.R.L., Ramamurthy, T.S., Shetb, A.: Estimation of impact-induced damage in CFRR laminates through ultrasonic imaging. *NDT E Int* **31**, 359–374 (1998)
6. Zhou, G.: The use of experimentally-determined impact force as a damage measure in impact damage resistance and tolerance of composite structures. *Compos Struct* **42**, 375–382 (1998)
7. Delfosse, D., Poursartip, A.: Energy-based approach to impact damage in CFRP laminates. *Composites Part A* **28**, 647–655 (1997)
8. Poe, C.C., Jackson W.C.: The use of impact force as a scale parameter for the impact response of composite laminates. *J Compos Tech Res*. **15** (1993)
9. Djordjevic, D.D.: Ultrasonic characterization of advanced composite materials, in: *The 10th International Conference of the Slovenian Society for Non-Destructive Testing*. (Ljubljana, Slovenia, 2009), pp. 45–75
10. Vary, A.: Acousto-ultrasonics. In: Summerscales, J. (ed.) *Non-Destructive Testing of Fibre-Reinforced Plastics Composites*, vol. 2, pp. 1–47. Elsevier Science Publishing, Essex (1990)
11. Polimeno, U., Meo, M., Almond, D.P., Angioni, S.L.: Detecting low velocity impact damage in composite plate using nonlinear acoustic/ultrasound methods. *Appl Compos Mater* **17**, 481–488 (2010)
12. T.J. Barden, D.P. Almond, M. Morbidini, P. Cawley, Advances in thermosonic for detecting impact damage in CFRP composites. BINDT conference (2005)
13. Hung, Y.Y., Ho, H.P.: Shearography: An optical measurement technique and applications. *Mater Sci Eng R Rep* **49**, 61–87 (2005)
14. Hung, Y.Y.: Shearography for non-destructive evaluation of composite structures. *Opt Lasers Eng* **24**, 161–182 (1996)
15. Huang, Y.H., Ng, S.P., Liu, L., Li, C.L., Chen, Y.S., Hung, Y.Y.: NDT&E using shearography with impulsive thermal stressing and clustering phase extraction. *Opt Lasers Eng* **47**, 774–781 (2009)
16. Pickering, S.G., Almond, D.P.: Comparison of the defect detection capabilities of flash thermography and vibration excitation shearography. *Insight-NDT Cond Monit* **52**, 1354–2575 (2010)
17. Ambu, R., Aymerich, F., Ginesu, F., Priolo, P.: Assessment of NDT interferometric techniques for impact damage detection in composite laminates. *Compos Sci Technol* **66**, 199–205 (2006)
18. R. Krupka, T. Walz, Industrial application of shearography for inspection of aircraft components. Proc. National Seminar on Non-Destructive Evaluation. Hyderabad, Dec. 7 (2006)
19. Steinchen, W., Yang, L.X., Kupfer, G., Mäkel, P.: Non-destructive testing of aerospace composite materials using digital shearography. *J Aerospace Eng* **212**, 21–30 (1998)
20. Newman, J.W., Lindberg, J.: Laser shearography of wind turbine blades. *Mat Eval* **68**, 828–837 (2010)
21. Růžek, R., Běhal, J.: Certification programme of airframe primary structure composite part with environmental simulation. *Int J Fatigue* **31**, 1073–1080 (2009)
22. Růžek, R., Lohonka, R., Jironč, J.: Ultrasonic C-Scan and shearography NDI techniques evaluation of impact defects identification. *NDT E Int* **39**, 132–142 (2006)
23. Hung, Y.Y., Chen, Y.S., Ng, S.P., Liu, L., Huang, Y.H., Luk, B.L.: Review and comparison of shearography and active thermography for nondestructive evaluation. *Mater Sci Eng R Rep* **64**, 73–112 (2009)

24. Amaro, A.M., Santos, J.B., Cirne, J.S.: Comparative study of different non-destructive testing techniques in the characterisation and quantification of the damage effects in carbon-epoxy laminates. *Insight* **46**, 559–565 (2004)
25. Findeis, D., Gryzagoridis, J.: A comparison of the capabilities of portable shearography and portable electronic speckle pattern interferometry. *Proc SPIE* **5393**, 45–49 (2004)
26. Okafor, A.C., Otieno, A.W., Dutta, A.: Detection and characterization of high/velocity impact damage in advanced composite plates using multi/sensing techniques. *Compos Struct* **54**, 289–297 (2001)
27. Cantwell, W.J., Morton, J.: Geometric effects in the low velocity impact response of CFRP. *Compos Struct* **12**, 756–758 (1989)
28. G. Guangping, Q. Yuwen, Quantitative analysis on sensitivity of shearography in NDT. in: *Proc. SPIE Vol. 4537*, ed. by X. Wu, Y. Qin, J. Fang, J. Ke (Third International Conference on Experimental Mechanics, 2002), pp. 341–344
29. Schoeppner, G.A., Abrate, S.: Delamination threshold loads for low velocity impact on composite laminates. *Composites Part A* **31**, 903–915 (2000)
30. Hirai, Y., Hamada, H., Kim, J.: Impact response of woven glass-fabric composites—II. Effect of temperature. *Compos Sci Technol* **58**, 119–128 (1998)
31. Hutchinson, J.W., Lu, T.J.: Laminate Delamination Due to Thermal Gradients. *J Eng Mater Technol* **117**, 386–391 (1995)
32. Hay, T.R., Wei, L., Rose, J.L.: Rapid Inspection of Composite Skin-Honeycomb Core Structures with Ultrasonic Guided Waves. *J Compos Mater* **37**, 929–939 (2003)